

Effect of laser radiation on the gamma activity of aqueous salt solutions containing ^{152}Eu

E.V. Barmina, A.V. Simakin, V.I. Stegailov, S.I. Tyutyunnikov,
G.A. Shafeev, I.A. Shcherbakov

Abstract. We report an experimental study of the effect of laser irradiation of aqueous salt solutions containing the ^{152}Eu isotope in the presence of nickel nanoparticles on the gamma activity of the isotope. Nickel nanoparticles are generated using laser ablation of the target in water and added to the radionuclide solution before irradiation. Two types of Nd:YAG lasers with a pulse duration of 10 ns and different repetition rates are used to irradiate the solutions. It is found that the ^{152}Eu activity as a result of repeated irradiation of solutions by a series of pulses decreases with each irradiation cycle. The obtained results are compared with data on the effect of maser radiation with a wavelength of 8 mm on the activity of the same isotope. Possible mechanisms of the effect of electromagnetic radiation on the ^{152}Eu gamma activity are discussed.

Keywords: gamma activity of isotopes, laser radiation, nanoparticle solutions.

1. Introduction

A number of papers reported the observation of effects of relatively low laser intensities (10^{10} – 10^{12} W cm⁻²) on the concentration of radionuclides, determined by the number of counts of the gamma-quanta accompanying beta decay [1–9]. In these studies, the activity of nuclides was determined before and after laser irradiation of solutions, which did not exclude the possibility of methodological errors associated with the geometry of measurements and the loss of solution on the cell walls. These deficiencies were subsequently eliminated by recording the gamma activity of nuclide solutions before, during, and after laser irradiation at invariable geometry. Changes in activity were observed in the presence of nanoparticles in a liquid, either formed during laser ablation of a metal target in the solution or added to the solution.

In the presence of nanoparticles in a liquid, the process of dissociation of water molecules under the action of laser breakdown in colloidal solutions of nanoparticles and laser ablation of targets in water actively occurs [10]. As a result of dis-

sociation, stable products are formed: molecular hydrogen and oxygen, as well as hydrogen peroxide. It was found that the yield of products depends on the concentration and type of the nanoparticle material. Thus, the maximum rate of hydrogen peroxide formation is observed in using nanoparticles of ferromagnetic materials (nickel, cobalt, etc.) [11–13]. Since in the interaction of laser radiation with solutions of radionuclides, as in the dissociation of a liquid, breakdown plasma arises, one can assume that the plasma properties, for example, the number of breakdowns per laser pulse, will be similar. In both cases, it is the laser breakdown of the solution that determines the change in the activity of radionuclides and the yield of liquid dissociation products. Earlier, the effect of electromagnetic radiation on the ^{152}Eu isotope has already been investigated when its salt was exposed to microwave radiation with a wavelength of 8 mm, while metal filings were admixed to the nuclide sample [14]. In the present work, we investigate the effect of laser irradiation of aqueous salt solutions containing ^{152}Eu with an addition of nickel nanoparticles, the concentration of which is optimal in terms of activity of this effect. Identification of similarities or differences between the microwave and laser effects on the ^{152}Eu radioactivity may help to draw some conclusions about the mechanism of this unusual phenomenon, i. e. the effect of electromagnetic radiation on the concentration of radionuclides.

2. Experimental

Nickel nanoparticles were prepared using laser ablation in liquid [15]. The radiation source was a fibre ytterbium laser with a pulse repetition rate of 20 kHz and a pulse duration of 100 ns. The laser beam was scanned over the surface of a nickel target immersed in Milli-Q water. The colloidal solution remaining in the cell after the ablation termination was analysed using a disk measuring centrifuge and a transmission electron microscope (TEM). Most of the particles are about 10 nm in size (Fig. 1). The TEM image shows that in addition to nanoparticles, there is also a diffuse halo surrounding them. Presumably, it consists of nickel hydroxide formed as a result of the chemical reaction of nickel with water at an elevated temperature during laser ablation of the target. The data obtained by centrifugation also make it possible to find the mass of nanoparticles in the test sample volume. A few minutes before the addition of $^{152}\text{EuCl}_3$ to the aqueous solution, a colloidal solution of nickel nanoparticles was placed in an ultrasonic bath for the destruction of nanoparticle aggregates. Such aggregates are easily formed, since nickel nanoparticles are magnetic.

Two types of lasers were used to irradiate europium salt solutions with the addition of nickel nanoparticles:

E.V. Barmina, A.V. Simakin, I.A. Shcherbakov Prokhorov General Physics Institute, Russian Academy of Sciences, ul. Vavilova 38, 119991 Moscow, Russia;

V.I. Stegailov, S.I. Tyutyunnikov Joint Institute for Nuclear Research, ul. Joliot-Curie 6, 141980 Dubna, Moscow region, Russia;

G.A. Shafeev Prokhorov General Physics Institute, Russian Academy of Sciences, ul. Vavilova 38, 119991 Moscow, Russia; National Research Nuclear University 'MEPhI', Kashirskoe shosse 31, 115409 Moscow, Russia; e-mail: shafeev@kapella.gpi.ru

Received 27 February 2019; revision received 10 May 2019
Kvantovaya Elektronika 49 (8) 784–787 (2019)
Translated by M.A. Monastyrskiy

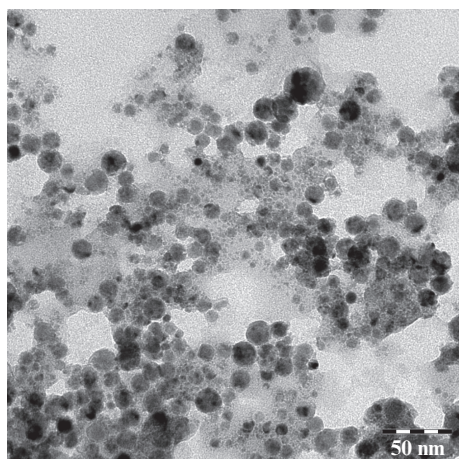


Figure 1. TEM image of nickel nanoparticles formed by laser ablation of a nickel target in water.

1. Nd:YAG laser with a wavelength of 1064 nm, a pulse duration of 10 ns, a pulse repetition rate of 10 kHz, and a pulse energy of 1.6 mJ.

2. Nd:YAG laser with a wavelength of 1064 nm, a pulse duration of 10 ns, a pulse repetition rate of 10 kHz, and a pulse energy of 700 mJ.

When the ^{152}Eu chloride solutions were exposed in the presence of nanoparticles, a laser beam with a pulse repetition rate of 10 kHz moved along a circular trajectory at a rate of 1300 mm s^{-1} using a galvo mirror system. The laser beam waist was located inside the cell with the solution at a distance of 2–3 mm from the surface of the entrance window (above it) and, when moving in a circle, formed a plasma ring visible to the naked eye. Laser radiation was focused from the bottom up with lenses or a lens with a focal length of 20–95 mm, depending on the laser type used. In the case of a laser with a pulse repetition rate of 10 Hz, the beam was not scanned.

The cell was cooled with running water, and so the heating of the entire volume of the solution during the laser exposure did not exceed several degrees. The cell was fixed at a distance of several millimetres from the sensitive part of the gamma-ray detector, but without mechanical contact with the latter. The liquid-nitrogen cooled detector based on ultrapure germanium (Canberra) had a relative recording efficiency of 30%. The geometry of activity measurements remained constant before, during, and after laser exposure. The numbers of counts were stored in the computer memory once per second, the signal accumulation time was selected so that the measurement error did not exceed 0.5%.

3. Results and discussion

Microphotographs of the plasma ring arising when the laser beam is scanned in the solution show that the plasma tracks left by individual laser pulses are not continuous (Fig. 2). The nanoparticles added to the solution are the centres of the laser breakdown and plasma formation. The number of breakdowns in each track fluctuates, which can be explained by the breakdown of the liquid on the nanoparticle aggregates. Each plasma formation is a microreactor in which water dissociates and decomposes into H_2 , O_2 and H_2O_2 under the action of electrons in the breakdown plasma. The same discrete struc-

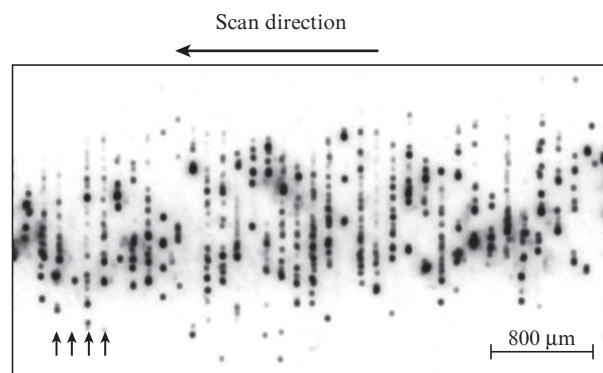


Figure 2. Negative microphotograph of laser-induced plasma obtained by irradiation of the ^{152}Eu solution with nickel nanoparticles by a train of laser pulses. Vertical arrows indicate plasma tracks formed by individual laser pulses in the laser beam waist. An Nd:YAG laser with a pulse duration of 10 ns, a repetition rate of 10 kHz, and a pulse energy of 1.6 mJ was used. The laser beam scanning velocity was 1.25 m s^{-1} .

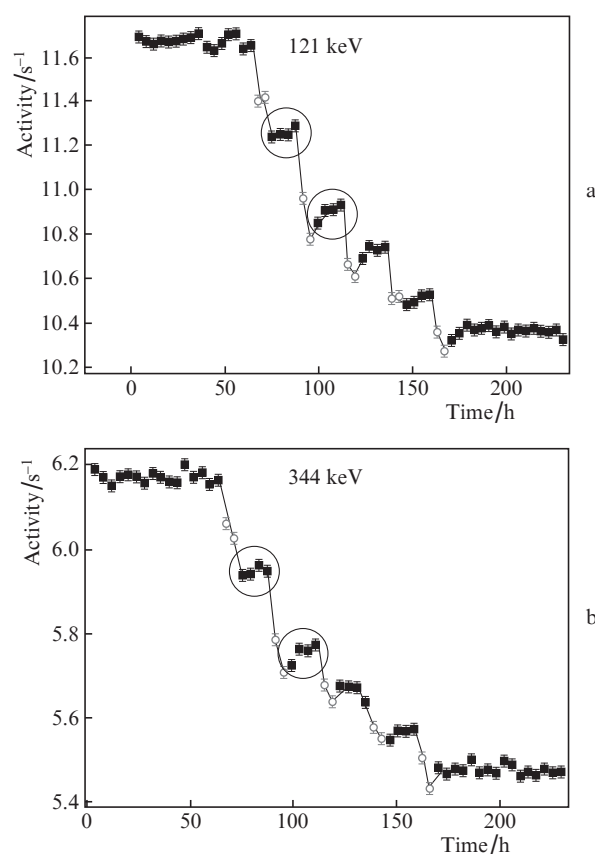


Figure 3. Evolution of the gamma activity of the ^{152}Eu solution on lines with energies of (a) 121 and (b) 344 keV with periodically renewed laser irradiation with a pulse duration of 10 ns. The black squares correspond to the time moments when the laser irradiation is absent, and the bright circles correspond to the time moments of irradiation. An Nd:YAG laser with a pulse energy of 700 mJ and a pulse repetition rate of 10 Hz was used. The concentration of nickel nanoparticles was $10 \mu\text{g mL}^{-1}$. The circles indicate the time intervals of partial restoration of the samples' activity in the absence of laser radiation.

ture of the breakdown plasma is observed in irradiation by another laser source with a pulse energy of 700 mJ.

If the ^{152}Eu aqua-ions are inside the plasma formation region, the laser radiation affects them, changing the sample activity. The results of such an exposure are presented in Figs 3 and 4.

The ^{152}Eu half-life is 13.537 years. From this state, the europium isotope with a $\sim 70\%$ probability as a result of the β^- -decay turns into a long-lived ^{152}Gd isotope (344 keV, α -active) and with a $\sim 30\%$ probability as a result of β^+ -decay turns into a long-lived ^{152}Sm isotope (121 keV, α -active). It should be noted that both decay channels have a total energy level of the ^{152}Eu nucleus. The sample activity was measured on a line with an energy of 121 keV at a decay of ^{152}Eu into ^{152}Sm and a line with an energy of 344 keV at a decay of ^{152}Eu into ^{152}Gd .

Figure 3 shows the gamma activity evolution of ^{152}Eu in a solution with the addition of nickel nanoparticles under nanosecond laser irradiation. The total laser irradiation time was 40 hours. This corresponds to 1.44×10^6 laser pulses at a repetition rate of 10 Hz. It is seen that under laser irradiation action of the solution the rate of gamma-quanta counts from the irradiated sample decreases. Before irradiation, this value is $A_0 = 11.6 \text{ s}^{-1}$, and after irradiation it amounts to $A_f = 10.3 \text{ s}^{-1}$ for lines with an energy of 121 keV. It should be noted that after the end of all cycles of laser irradiation of the solution, the A_f activity remains constant and does not return to the values observed before the laser exposure. The relative change in the $(A_0 - A_f)/A_0$ activity on a line with an energy of 121 keV is $11.2\% \pm 0.2\%$, and on a line with an energy of 344 keV this change constitutes $11.3\% \pm 0.2\%$, i.e. almost the same for both lines.

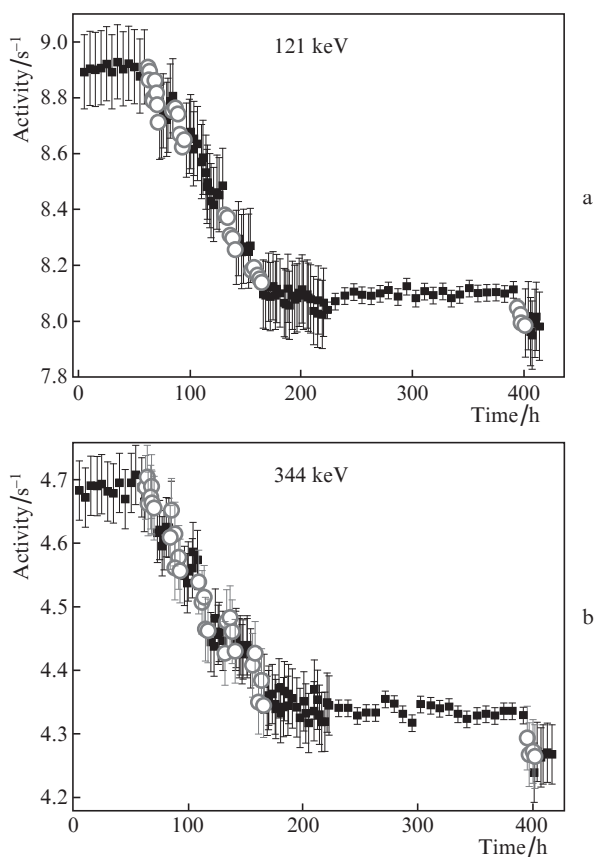


Figure 4. Same as in Fig. 3 but using an Nd:YAG laser with a pulse energy of 1.6 mJ and a pulse repetition rate of 10 kHz.

Similar dynamics in the ^{152}Eu activity reduction is observed when nanosecond pulses are applied to the solution at a pulse repetition rate of 10 kHz and a pulse energy of 1.6 mJ (Fig. 4). The total laser irradiation time was 57 hours. This corresponds to 2.05×10^9 laser pulses at a repetition rate of 10 kHz. The relative change in the $(A_0 - A_f)/A_0$ activity for the entire irradiation time was $10.1\% \pm 0.2\%$ on a line with an energy of 121 keV and $8.9\% \pm 0.2\%$ on a line with an energy of 344 keV.

Figures 3 and 4 show that laser irradiation of the aqueous solution containing ^{152}Eu when nickel nanoparticles are added leads to a change in its activity. A significant difference in the activity change rates is clearly visible – with laser irradiation it is significantly greater than without it. Of course, this does not mean a change in the isotope's half-life, since the gamma radiation excess on the lines with energies of 121 and 344 keV is absent, but only implies a decrease in the isotope content (concentration) under laser irradiation. The characteristic time of reducing the content by half, estimated from the activity curve slope, is 30 days.

It is of interest to note that a change in the ^{152}Eu activity was also observed when the focused microwave radiation was applied to its sample in the form of dry powder, although there are several qualitative differences. Immediately after the microwave exposure, the sample activity decreased, then returned to the original value and for some time (several days) was even greater [14]. The return of activity to the original value occurred after a few days later. In the case of laser irradiation of the solution of this nuclide, the activity increases after the end of laser irradiation to the initial value not completely, but partially. The decrease in the $(A_0 - A_f)/A_0$ activity after laser irradiation is an order of magnitude greater than under microwave exposure and does not change after the end of laser irradiation during subsequent observations [14].

The daughter products of ^{152}Eu decay, i.e. ^{152}Gd and ^{152}Sm isotopes, are also rare-earth elements, whose ion absorption spectra in water are well known. The peak intensity ratio of these ions (absorption peaks at wavelengths of 273 and 401 nm, respectively) before and after laser irradiation could have led to a conclusion about the equilibrium of the two ^{152}Eu decay channels. It has not yet been possible to confirm the appearance of daughter products by their absorption spectra because of their low expected concentration (of the order of units of picograms per millilitre of solution). With an acceptable signal-to-noise ratio, only the absorption of the Eu ion itself at a wavelength of 395 nm was recorded.

On the other hand, a comparison of the relative changes in the $(A_0 - A_f)/A_0$ activities for the two lines shows that the irradiation of ^{152}Eu solutions by laser radiation with a higher pulse energy (700 mJ) leads to almost the same change in the relative activities for both their gamma-spectrum lines associated with ^{152}Gd and ^{152}Sm . On the contrary, under irradiation with a pulse energy of 1.6 mJ, the relative activity change is greater for a line with an energy of 121 keV (decay in ^{152}Sm) than for a line with an energy of 344 keV (decay in ^{152}Gd). Thus, we may conclude that with such a laser action, the equilibrium of the ^{152}Eu decay channels is shifted towards the positron β^+ -decay.

It seems highly probable that the observed changes in the ^{152}Eu activity both at laser and microwave exposure can be attributed to the accumulation of isomeric states of the ^{152}Eu nuclei under electromagnetic action [14, 16]. Presumably, the nucleus disturbance is caused by the high-power electric field of the laser (microwave) beam, amplified by plasmon reso-

nance on the nanoparticle aggregates. Indeed, the electric field amplification on the aggregates of metal nanoparticles significantly exceeds the amplification on individual nanoparticles, so that in this case the field can increase by 10^3 – 10^4 times [17, 18]. Nanoparticle aggregates are considered to be particles located at a mutual distance being much smaller than their radius. The greatest electric field value is attained in the gap between the particles. Under the conditions of this work, such aggregates can occur randomly due to fluctuations in the density of nanoparticles. Then, at a laser radiation intensity of $\sim 10^{12}$ W cm $^{-2}$ near the aggregates, the effective intensity may reach 10^{18} W cm $^{-2}$. The electric field at this intensity is comparable to the intra-atomic fields and can have a noticeable effect on the electronic shell around the nuclei. In turn, electronic shell rearrangement can affect the nucleus and change its state. With such an intensity, it is possible to accelerate electrons and ions in laser plasma to high energies exceeding the thresholds of a number of nuclear reactions [19].

Another possible mechanism of the observed process is the transition of the ^{152}Eu nucleus to the isomeric level which is separated from the known energy level by several kiloelectronvolts. This type of splitting is observed in heavy nuclei, and the transition between levels of close energies can occur under laser plasma action. This was demonstrated by the example of a metastable ^{186}Re nucleus exposed to laser radiation from the Iskra-5 installation [20]. The presence of fine splitting of the nucleus energy levels is difficult to establish in beam experiments, and many isomeric levels of heavy nuclei, including the ^{152}Eu nucleus, remain unknown.

4. Conclusions

It has been experimentally shown that the processes of changing the ionic composition of radionuclide solutions and reducing their radioactivity during laser irradiation occur simultaneously, accompanying each other. The results of this work allow us to compare the efficiency of various laser sources when the concentration of radionuclides varies. In using the considered laser sources, a comparable change in the activity of the ^{152}Eu samples by about 10% was obtained. At a pulse energy of 1.6 mJ, this required a larger (by three orders of magnitude) number of laser pulses than that at an energy of 700 mJ for the same duration of laser pulses (~ 10 ns). On the other hand, the ^{152}Eu concentration is small; therefore, the probability of its ions getting into isolated plasma clots arising randomly is small as well. Therefore, to increase the efficiency of reducing the activity of nuclides under laser exposure, it is necessary to use lasers with a high pulse energy and high pulse repetition rate.

Acknowledgements. The authors express their gratitude to V.B. Loshchenov for his assistance in conducting optical measurements, Common Use Center of Prokhorov General Physics Institute, and to O.V. Uvarov for electron microscopy of nanoparticles.

The work has been performed as part of the State Task (AAAA-A18-118021390190-1 topic) and in the framework of the NRNU ‘MEPhI’ Competitiveness Enhancement Programme (Contract No.02.a03.21.005, 27 August 2013), and partially supported by the Russian Foundation for Basic Research (Grant Nos 18-52-70012_e_Asia_a and 19-02-00061_a), and supported by the Presidium of the Russian Academy of

Sciences (Photonic Technologies in Probing Inhomogeneous Media and Biological Objects Programme No. 5).

References

1. Simakin A.V., Shafeev G.A. *J. Optoelectron. Adv. Mater.*, **12** (3), 432 (2010).
2. Simakin A.V., Shafeev G.A. *Appl. Phys. A*, **101**, 199 (2010).
3. Simakin A.V., Shafeev G.A. *Phys. Wave Phenom.*, **19** (1), 30 (2011).
4. Simakin A.V., Shafeev G.A. *Quantum Electron.*, **41** (7), 614 (2011) [*Kvantovaya Elektron.*, **41** (7), 614 (2011)].
5. Simakin A.V., Shafeev G.A. *Phys. Wave Phenom.*, **21** (1), 31 (2013).
6. Shafeev G.A., in *Uranium: Characteristics, Occurrence and Human Exposure* (New York: Novapublishers Inc., 2012) pp 117–153.
7. Barmina E.V., Simakin A.V., Shafeev G.A. *Quantum Electron.*, **44** (8), 791 (2014) [*Kvantovaya Elektron.*, **44** (8), 791 (2014)].
8. Barmina E.V., Simakin A.V., Stegailov V.I., Tyutyunnikov S.I., Shafeev G.A., Shcherbakov I.A. *Quantum Electron.*, **47** (7), 627 (2017) [*Kvantovaya Elektron.*, **47** (7), 627 (2017)].
9. Andreev S.N., Barmina E.V., Kalinnikov V.G., Simakin A.V., Smirnov A.A., Stegailov V.I., Tyutyunnikov S.I., Shafeev G.A., Shcherbakov I.A. *Phys. Part. Nucl. Lett.*, **14** (6), 894 (2017).
10. Kalus M.R., Bärsch N., Streubel R., Gökce E., Barcikowski S., Gökce B. *Phys. Chem. Chem. Phys.*, **19** (10), 7112 (2017).
11. Barmina E.V., Simakin A.V., Shafeev G.A. *Chem. Phys. Lett.*, **678**, 192 (2017).
12. Sukhov I.A., Shafeev G.A., Barmina E.V., Simakin A.V., Voronov V.V., Uvarov O.V. *Quantum Electron.*, **47** (6), 533 (2017) [*Kvantovaya Elektron.*, **47** (6), 533 (2017)].
13. Barmina E.V., Gudkov S.V., Simakin A.V., Shafeev G.A. *J. Laser Micro/Nanoeng.*, **12** (3), 254 (2017).
14. Gonz Z., Kalinnikov V.G., Kaminsky A.K., Sedykh S.N., Smirnov A.A., Stegailov V.I., Sushkov A.V., Tyutyunnikov S.I. *Proc. of the 9th Int. Workshop ‘Strong Microwaves and Terahertz Waves: Sources and Applications’* (N.Novgorod, 2014) pp 84, 85.
15. Kazakevich P.V., Simakin A.V., Voronov V.V., Shafeev G.A. *Appl. Surf. Sci.*, **252**, 4373 (2006).
16. Andreev S.N., Barmina E.V., Kaminsky A.K., Sedykh S.N., Shafeev G.A., Shcherbakov I.A., Simakin A.V., Stegailov V.I., Tyutyunnikov S.I. *Proc. of the 10th Int. Workshop ‘Strong Microwaves and Terahertz Waves: Sources and Applications’* (N.Novgorod–Moscow, 2017) pp 88, 89.
17. Hao E., Schatz G.C. *J. Chem. Phys.*, **120** (1), 357 (2004).
18. Blanco L.A., García de Abajo F.J. *J. Quant. Spectrosc. Radiat. Transfer.*, **89**, 37 (2004).
19. Krainov V.P. *Yadernaya Fiz.*, **74** (10), 1438 (2011).
20. Es’man A.A., Kulakov M.A., Larin D.E., Tkachev G.V. *Vopr. At. Nauki Tekh., Ser. Teor. Priklad. Fiz.*, (4), 43 (2017).